Quantum stirring of particles in closed devices

Gilad Rosenberg and Doron Cohen

Department of Physics, Ben-Gurion University, Beer-Sheva 84105, Israel

Abstract. We study the quantum analog of stirring of water inside a cup using a spoon. This can be regarded as a prototype example for quantum pumping in closed devices. The current in the device is induced by translating a scatterer. Its calculation is done using the Kubo formula approach. The transported charge is expressed as a line integral that encircles chains of Dirac monopoles. For simple systems the results turn out to be counter intuitive: e.g. as we move a small scatterer "forward" the current is induced "backwards". One should realize that the route towards quantum-classical correspondence has to do with "quantum chaos" considerations, and hence assumes greater complexity of the device. We also point out the relation to the familiar S matrix formalism which is used to analyze quantum pumping in open geometries.

1. Introduction

Consider a closed ring that contains particles (Fig.1a). Assume that one wants to create a current in this ring. If the particles are charged then one way to do it is by creating an electro motive force (EMF). This can be induced by varying an Aharonov-Bohm flux Φ , such that by Faraday's law EMF = $-\dot{\Phi}$. But there is another way to create a current that does not involve EMF, and hence does not assume charged particles. The idea is to change in time the scalar potential $V(r; X_1(t), X_2(t))$. Here r is the coordinate of a representative particle in the ring, while X_1 and X_2 are some control parameters. By making a cycle in the (X_1, X_2) space we can push non-zero net charge Q through the system. Thus an "AC driving" gives rise to a "DC" component in the current. This is known in the literature as "quantum pumping".

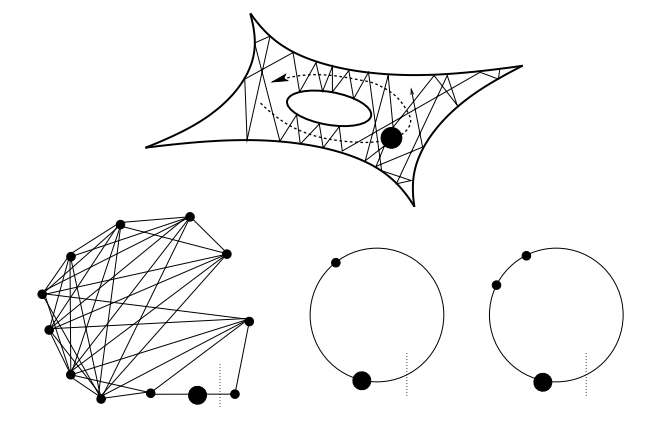


Fig.1. Models for the analysis of quantum stirring. (a) Upper panel: A scatterer (big black dot) is translated inside a Sinai billiard. A chaotic trajectory of a representative particle in this billiard is illustrated. (b) Lower panels: Network models for quantum stirring. The scatterer (big black dot) is translated along one of the bonds. The vertical dotted line is the section through which the current is measured. From left to right: chaotic network; double barrier model; triple barrier model.

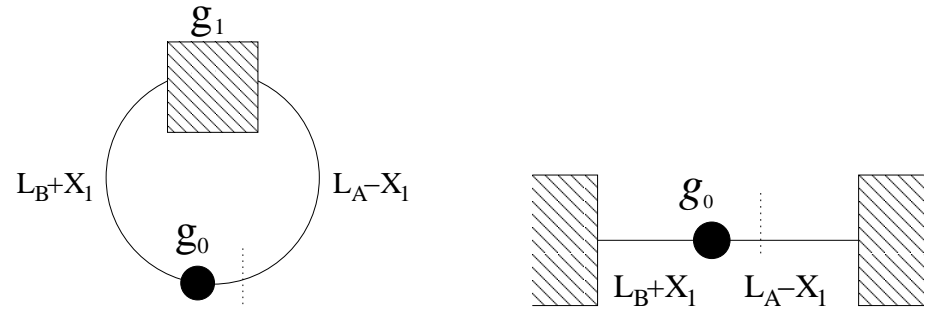


Fig.2. (a) Left panel: A schematic representation of the network model. The vertical dotted line is the section through which the current is measured. The moving scatterer is indicated by its transmission g_0 , while X_1 is its displacement along the bond. (b) Right panel: The corresponding open geometry where the left and right leads are connected to reservoirs with the same chemical potentials.

In this paper we would like to consider a prototype pumping problem, which we call "quantum stirring". It is the simplest scheme to create a current with a non-vanishing DC component. Referring to Fig.2 we define X_1 as the location of a scatterer, while X_2 is its "size". By "size" we mean either the cross section or the reflection coefficient. One can regard the scatterer as a "piston" or as a "spoon" with which it is possible to "push" the particles. A prototype example for a pumping cycle is illustrated in Fig.3. During the main stage of the cycle the scatterer is translated to the right a distance ΔX_1 . Consequently a charge Q is transported. In the second stage the size of the scatterer is "lowered", and it is displaced back to its original location, where its original "size" is restored. By repeating this cycle many times we can create a current with a DC component.

In the following analysis we assume that the system consists of non-interacting spinless particles. All the particles have (formally) charge e, even if they are not actually charged. We assume that there is no magnetic field in the system. Still, for the sake of a later mathematical formulation, it is convenient to introduce a third parameter $X_3 = \Phi$, where Φ is an Aharonv-Bohm flux. The pumping cycle in the (X_1, X_2, X_3) space is illustrated in Fig.3.

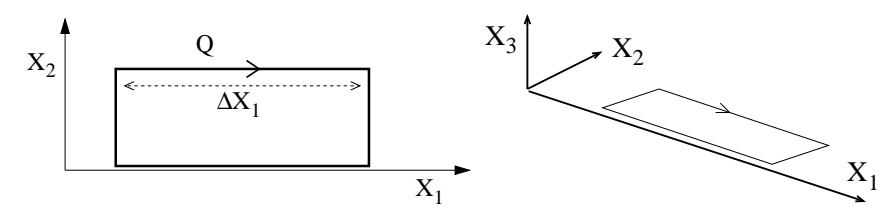


Fig.3. A prototype example for a pumping cycle. During the main stage of the cycle the scatterer is translated to the right a distance ΔX_1 . Consequently a charge Q is transported. (a) Left panel: The pumping cycle in the 2-dimensional (X_1, X_2) plane. (b) Right panel: The same pumping cycle in the three dimensional (X_1, X_2, X_3) space, where $X_3 = \Phi$ is the Aharonov Bohm flux via the ring.

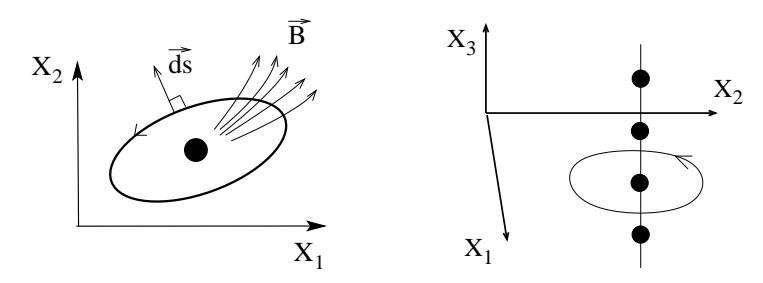


Fig.4. (a) Left panel: The calculation of the charge Q is a line integral over G that can be regarded as a calculation of the flux of B via a two dimensional curve. $d\vec{s}$ is a normal vector to the pumping cycle. The black dot in the middle symbolizes the presence of "magnetic charge" which is characterized by a density $\sigma(X_1, X_2)$. In the quantum mechanical analysis this should be understood as the density of "Dirac chains". (b) Right panel: In the embedding (X_1, X_2, X_3) space the magnetic charge is organized as vertical charged chains. Each chain consists of "Dirac monopoles" which are located at \vec{X} points where an occupied level has a degeneracy with a nearby level. The ellipse represents a possible pumping cycle that may encircle either one or many chains.

1.1. Linear response theory and the Dirac chains picture

We are going to analyze the stirring problem within the framework of linear response theory. If we have EMF then we expect to get in the DC limit Ohm law $I = -G\dot{\Phi}$, while if we change slowly either X_1 or X_2 we expect to get in the DC limit $I = -G^1\dot{X}_1$ or $I = -G^2\dot{X}_2$ respectively. So in general we can write

$$Q = \oint_{\text{cycle}} Idt = -\oint (G^1 dX_1 + G^2 dX_2) = \oint \mathbf{B} \cdot d\mathbf{\hat{s}} = \iint \sigma(X_1, X_2) dX_1 dX_2$$
 (1)

In the second expression we define the normal vector $\vec{ds} = (dX_2, -dX_1)$ and use the notations $\mathbf{B}_1 = -G^2$ and $\mathbf{B}_2 = G^1$. See Fig.4a for an illustration. The third expression is obtained via the two dimensional version of the divergence theorem. If we regard \mathbf{B} as a fictitious magnetic field, then σ is the two dimensional density of magnetic charge.

It turns out that in the strict adiabatic limit the vector field \mathbf{B} is related to the theory of Berry phase [1, 2]. The formulation of this relation is as follows. Assume that the system is adiabatically cycled in the (X_1, X_2, X_3) space. In such case the Berry phase can be calculated as a line integral over a "vector potential" (also called "1 form") \mathbf{A} . This can be converted by the Stokes theorem into a surface integral over a "magnetic field" (also called "2 form") \mathbf{B} . The \mathbf{B} field is defined as the "rotor" of \mathbf{A} . It is a divergence-less field but it can have singularities which are known as "Dirac monopoles". These monopoles are located at \vec{X} points where an occupied energy level has a degeneracy with a nearby level. Because of $\Phi \mapsto \Phi + (2\pi\hbar/e)$ gauge invariance the Dirac monopoles form vertical chains as illustrated in Fig.4b. Hence we have a distribution of what we call "Dirac chains" [3, 4], which is characterized by a density $\sigma(X_1, X_2)$.

1.2. Background and objectives

Most of the literature about quantum pumping deals with the open geometry of Fig.2b. The most popular approach is the *S*-scattering formalism which leads to the Büttiker, Prêtre and Thomas (BPT) formula [5, 6] for the generalized conductance *G*. The BPT formula, is essentially a generalization of the Landauer formula. In previous publications [7, 4] we have demonstrated that the BPT formula can be regarded as a special limit of the Kubo formula. Our Kubo formula approach to pumping [3, 8] leads to "level by level" understanding of the pumping process, and allows to incorporate easily non-adiabatic and environmental effects. In the strict adiabatic limit it reduces in a transparent way to the theory of adiabatic transport [9, 10], also known as "geometric magnetism [2]. On the other hand, in the non-adiabatic(!) "DC limit" of an open geometry it reduces to the *S* matrix picture, hence resolving some puzzles that had emerged in older publications.

The question "how much charge is pushed by translating a scatterer" has been addressed in Ref.[11] in the case of an open geometry using the BPT formula. We have addressed the corresponding problem of quantum stirring in closed geometry in a previous short publication [12], but the connection with the Dirac chains picture has not been illuminated. Furthermore, in [12] only the quantum chaos limit was considered.

In the present publication we put an emphasis on clarifying the route towards quantum-classical correspondence (QCC). We shall see that quantum mechanical effects are pronounced in *simple* systems. As the system becomes more chaotic QCC emerges. The Dirac chains picture leads to new insights regarding the route towards QCC. These insights are easily missed if we stick to the formal Green function calculation of our earlier work [12]. From the above it should be clear that the main objectives of the present study are:

- Derivation of a classical formula for Q (assuming a stochastic picture).
- Derivation of a quantum result for Q using the Dirac chains picture.
- \bullet Exposing some counter-intuitive results for Q in the case of the simplest models.
- Illuminating the route towards QCC as we go from "simple" to "chaotic" systems.

We note that in [12] we have presented the classical formula for Q without the derivation.

1.3. Physical motivation and experimental feasibility

In the previous section we have explained the theoretical motivations for dealing with the stirring problem. In the present section we would like to further discuss the practicality of this line of study, and the feasibility of actual experiments.

It is quite clear that the main focus of today's experiments is on *open* devices (with leads), whereas our interest is in *closed* devices. Our believe is that "wireless" mesoscopic or molecular size devices are going to be important building blocks of future "quantum electronics". This is of course a vision that people may doubt. However, on the scientific side our task is to analyze its feasibility.

It is possible to fabricate closed mesoscopic rings, and to measure the persistent or the induced currents. Experiments with closed devices have been performed already 10 years ago. As an example we mention Ref.[13] where a large array of rings has been fabricated. The current measurement has been achieved by coupling the rings to a highly sensitive electromagnetic superconducting micro-resonator.

The conceptually simplest way to drive a current is by inducing an electro motive force (EMF). In the setup of Ref.[13] the EMF has been induced by a "wire" that spirals on top of the array. In our view an attractive alternative option would be to induce currents by changing

gate voltages so as to induce stirring. The advantage of such a possibility for the purpose of integrating wireless devices in future quantum electronics is quite obvious: It is much easier to control gate voltages than fluxes of magnetic field.

As far as *electronic devices* are concerned there is no question about the feasibility of realizing quantum stirring by manipulating gate voltages, and measuring the electrical currents. But we would like to argue that such possibility is open also in case of *neutral atoms*. It is well known that "billiards" that confine cold atoms can be realized and manipulated [14, 15]. Furthermore, there is no question regarding the possibility of creating a "moving" optical barrier so as to create a stirring effect. There are variety of techniques to measure the induced neutral currents. For example one can exploit the Doppler effect at the perpendicular direction, which is known as the rotational frequency shift [16].

There is one more issue which might be of relevance in case of an actual experiment. The Kubo formalism assumes that the system settles into a steady state, whereas the preparation in case of an actual experiment is not very well controlled. We would like to argue that the results of the linear response analysis are quite robust. This issue is discussed in section 4 of Ref.[17]: What we get for Q in the Kubo analysis is not merely a formal result, but rather a prediction that has an actual physical significance.

1.4. Outline

In the first part of this paper we review the result for G in the case of an open system using the BPT formula. Then we present two equivalent derivations of the corresponding *classical* result in the case of a closed geometry. We use the term "classical" in the Boltzmann sense. This means that interference within the ring is neglected, while the reflection by the scatterers ("cross section") is calculated quantum mechanically. The first derivation is based on a direct solution of a master equation, while the second is a straightforward application of the Kubo formula. The classical calculation implies an expression for the density $\sigma(X_1, X_2)$ of the monopoles. The BPT formula implies $\sigma(X_1, X_2)$ that can be regarded as a special case of this calculation.

In the second part of this paper we turn to the quantum mechanical analysis. As a preliminary stage we discuss the general conditions for having a degeneracy point \vec{X} in the case of a one dimensional ring. Then we review how the pumped charge Q can be estimated by calculating a line integral that encircles "Dirac chains". Thus we realize that we have to figure out what the distribution $\sigma(X_1, X_2)$ of these chains looks like. Specifically, we consider the model systems that are illustrated in Fig.1, and schematically in Fig.2. The simplest is a ring where both g_1 and g_0 are modeled as delta barriers. The result for Q is quite remote from the classical expectation. Consequently we try to figure out what happens to $\sigma(X_1, X_2)$ as the system becomes more complex: First we add a second fixed barrier, and finally we consider what happens in the case of a "chaotic" barrier which is modeled using random matrix theory. We make it clear that the route to the classical limit is intimately related to so called "quantum chaos" considerations.

2. Pushing particles in an open geometry

Let us consider the model of Fig.2b, where we have a scatterer within a single mode wire which is connected to two reservoirs with the same chemical potential. In this section we assume non-interacting spinless electrons and zero temperature Fermi occupation. The scatterer is described by

$$V(r; X_1, X_2) = X_2 \delta(r - X_1) \tag{2}$$

Hence, for some fixed values of X_1 and X_2 its transmission is

$$g_0(X_2) = \left[1 + \left(\frac{\mathsf{m}}{\hbar^2 k_{\scriptscriptstyle F}} X_2\right)^2\right]^{-1} \tag{3}$$

where m is the mass of the particle and k_F is the Fermi momentum. From now on we work with units such that $\hbar = 1$. The S matrix of the scattering region can be written in the general form

$$\mathbf{S} = e^{i\gamma} \begin{pmatrix} i\sqrt{1 - g}e^{i\alpha} & \sqrt{g}e^{-i\phi} \\ \sqrt{g}e^{i\phi} & i\sqrt{1 - g}e^{-i\alpha} \end{pmatrix}$$
(4)

where γ is the total phase shift, α is the reflection phase shift, and $\phi = e\Phi/\hbar$ represents the flux which we assume to be zero. In the setup of Fig. 2b the length of the right lead is $L_A - X_1$ and the length of the left lead is $L_B + X_1$. Hence

$$g = g_0 \tag{5}$$

$$\gamma = k_{\rm F}(L_A + L_B) - \arctan\left(\frac{\mathsf{m}}{\hbar^2 k_{\rm F}} X_2\right) \tag{6}$$

$$\alpha = k_{\rm F}(L_A - L_B) - 2k_{\rm F}X_1 \tag{7}$$

Now that we know the dependence of the **S** matrix on the parameters (X_1, X_2) , the calculation of G is quite straightforward. We use the BPT formula

$$G^{j} = \frac{e}{2\pi i} \operatorname{trace}\left(P_{\text{lead}} \frac{\partial S}{\partial X_{j}} S^{\dagger}\right) \tag{8}$$

where P_{lead} projects on the channels of the lead where the current is measured. As indicated in Fig.2b the current is measured via a section which is located on the right lead. Using the BPT formula we get

$$G^{1} = -(1 - g_{0}) \frac{e}{\pi} k_{F} \tag{9}$$

$$G^2 = -g_0 \frac{e}{4\pi\hbar v_{\rm F}} \tag{10}$$

where v_F is the Fermi velocity corresponding to k_F . The result for G^1 is our main interest. It has been discussed in Ref.[11], where the term "snow plow" has been coined in order to describe its physical interpretation. Namely, for zero temperature Fermi occupation the density of electrons in the wire is k_F/π . Therefore the number of electrons that are pushed by the scatterer is $dN = (k_F/\pi) \times dX_1$. If the transmission of the scatterer is not zero, some of the electrons pass through it and consequently we have to multiply dN by the reflection probability $1 - g_0$.

3. Stirring of particles in a closed geometry

Let us consider the model of Fig.2a, where the system is closed. We assume that the transmission of the ring without the moving scatterer is g_1^{cl} , while the transmission of the scatterer itself is g_0 . In the following two subsections we shall present two optional derivations of the "classical" result for G. We use the term "classical" in the Boltzmann sense. Namely, we regard the scattering from either g_1^{cl} or g_0 as a stochastic process. Thus interference within the arms of the ring is not taken into account. For sake of comparison with the BPT-based result we still assume zero temperature Fermi occupation (while in later sections we shall allow any arbitrary occupation). Within this framework we obtain:

$$G^{1} = -\left[\frac{(1-g_{0})g_{1}^{cl}}{g_{0} + g_{1}^{cl} - 2g_{0}g_{1}^{cl}}\right] \frac{e}{\pi} k_{F}$$
(11)

$$G^{2} = -\left[\frac{(1-g_{1}^{cl})g_{0}}{g_{0} + g_{1}^{cl} - 2g_{0}g_{1}^{cl}}\right] \frac{e}{4\pi\hbar\nu_{F}}$$
(12)

We note that the amount of charge which is pushed by translating a scatterer a distance ΔX_1 can also be written as [12]

$$Q = -G^1 \Delta X_1 = \left[\frac{1 - g_0}{g_0} \right] \left[\frac{g_T}{1 - g_T} \right] \frac{e}{\pi} k_F \times \Delta X_1$$
 (13)

where g_T is the overall transmission of the ring (including the moving scatterer) if it were opened:

$$\left[\frac{1-g_T}{g_T}\right] = \left[\frac{1-g_0}{g_0}\right] + \left[\frac{1-g_1^{cl}}{g_1^{cl}}\right] \tag{14}$$

As expected the charge Q which is transported as a result of an X_1 displacement depends in a monotonic way on the reflection coefficient $1 - g_0$. It monotonically increases from zero, and attains half of its maximal value for $g_0 = g_1^{cl}$. A plot of Q versus the "size" of the scatterer is presented in Fig. 5 for three representative values of g_1^{cl} . We also plot Q against X_2 , assuming that the scatterer is modeled as a delta function.

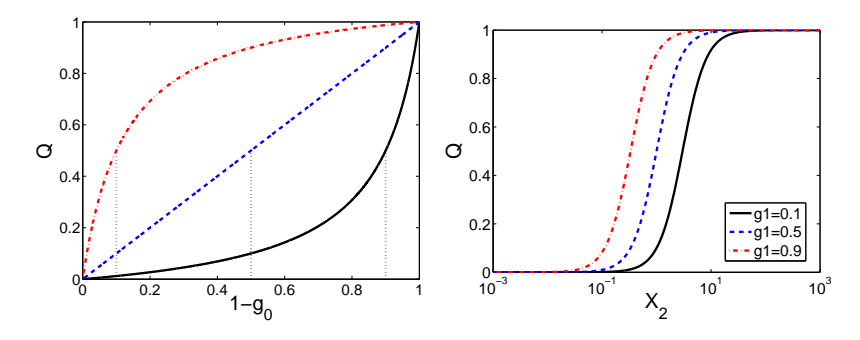


Fig.5. Plots of Q as a function of the "size" of the scatterer. We use arbitrary units such that Q=1 in the maximum. (a) Left panel: Q is plotted against the reflection coefficient $(1-g_0)$ for $g_1^{cl}=0.1$, for $g_1^{cl}=0.5$, and for $g_1^{cl}=0.9$. The dotted lines highlight that Q for $g_0=g_1^{cl}$ is half its maximum value. Note that the BPT based result corresponds to $g_1^{cl}=0.5$. (b) Right panel: Here Q is plotted against X_2 assuming that the scatterer is a delta function, and setting $\mathbf{m}/(\hbar^2 k_{\mathrm{F}})=1$.

It is important to realize that the result for an open geometry is formally a special case corresponding to $g_1^{cl} = 1/2$. This value of g_1^{cl} means that memory is completely lost once a particle is scattered by the "surroundings". Namely, if $g_1^{cl} = 1/2$ then after a collision a particle has equal probability to go in either direction, and any information about its initial direction is lost. This observation generalizes our discussion in Ref. [18] regarding the relation between the Kubo and the Landauer conductance.

The classical expression for G implies the following result for the density $\sigma(X_1, X_2)$, which is illustrated in Fig.6.

$$\sigma(X_1, X_2) = \frac{d\mathbf{B}_2}{dX_2} = -\frac{e\mathbf{m}}{\pi\hbar^2} \frac{2(1 - g_1^{cl})g_1^{cl}}{\left[1 + \left(\left(\frac{\mathbf{m}}{\hbar^2 k_F} X_2\right)^2 - 1\right)g_1^{cl}\right]^2} \left(\frac{\mathbf{m}}{\hbar^2 k_F} X_2\right)$$
(15)

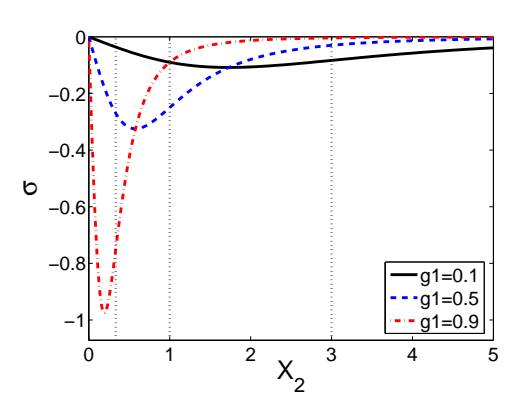


Fig.6. The classically deduced density σ as a function of X_2 for $g_1^{cl} = 0.1$, for $g_1^{cl} = 0.5$, and for $g_1^{cl} = 0.9$. We use arbitrary units for σ , and set $m/(\hbar^2 k_F) = 1$. The dotted vertical lines correspond to the median X_2 values which are determined by the equation $g_0(X_2) = g_1^{cl}$.

In the following sections we give two optional derivations of the classical result. The first derivation is based on a physically appealing master equation approach, in the spirit of the Boltzmann equation. The second derivation is a straightforward application of the Kubo formula. The calculation is done for G^1 and can be easily modified in order to get G^2 . The advantage of the Kubo formula approach is that it can be generalized to the quantum mechanical case, and it allows the incorporation of non-adiabatic and environmental effects.

4. Classical derivation using a master equation

We consider a ring with two scatterers: a moving scatterer g_0 whose velocity is \dot{X} , and a fixed scatterer g_1 . A collision of a particle with the moving scatterer implies that its velocity is changed $v \mapsto v \pm 2\dot{X}$, where the sign depends on whether the collision is from the right or from the left. The associated change in the kinetic energy is $E \mapsto E \pm 2 \text{mv} \dot{X} + O(\dot{X}^2)$ respectively. There are two regions (x < 0 and x > 0) on the two sides of the g_0 scatterer. Accordingly we have four distribution functions that satisfy the following balance equations:

$$\frac{\partial \rho_{+}^{\rightarrow}}{\partial t} = -[\rho_{+}^{\rightarrow} v] + g_{0}[\rho_{-}^{\rightarrow} v] + (1 - g_{0})[\rho_{+}^{\leftarrow} v]_{E-2m\nu\dot{X}}$$
(16)

$$\frac{\partial \rho_{+}^{\rightarrow}}{\partial t} = -[\rho_{+}^{\rightarrow} v] + g_{0} [\rho_{-}^{\rightarrow} v] + (1 - g_{0}) [\rho_{+}^{\leftarrow} v]_{E-2\mathsf{m}\nu\dot{X}}$$

$$\frac{\partial \rho_{+}^{\leftarrow}}{\partial t} = -[\rho_{+}^{\leftarrow} v] + g_{1} [\rho_{-}^{\leftarrow} v] + (1 - g_{1}) [\rho_{+}^{\rightarrow} v]$$
(16)

$$\frac{\partial \rho_{-}^{\rightarrow}}{\partial t} = -\left[\rho_{-}^{\rightarrow}v\right] + g_{0}\left[\rho_{+}^{\rightarrow}v\right] + (1 - g_{0})\left[\rho_{-}^{\leftarrow}v\right]$$

$$\tag{18}$$

$$\frac{\partial \rho_{-}^{\leftarrow}}{\partial t} = -[\rho_{-}^{\leftarrow} v] + g_1 [\rho_{+}^{\leftarrow} v] + (1 - g_1) [\rho_{-}^{\rightarrow} v]_{E+2m\nu\dot{X}}$$
(19)

The zero order solution in \dot{X} is to have all the four distribution functions equal to some arbitrary function f(E). In the presence of driving, assuming that the system has reached a steady state, we still have to satisfy the two \dot{X} -free equations, leading to

$$\rho_{+}^{\leftarrow} = g_{1}\rho_{-}^{\leftarrow} + (1 - g_{1})\rho_{+}^{\rightarrow} \tag{20}$$

$$\rho_{-}^{\rightarrow} = g_{1}\rho_{+}^{\rightarrow} + (1 - g_{1})\rho_{-}^{\leftarrow} \tag{21}$$

Substitution into the two other equations leads after linearization to

$$\rho_{+}^{\rightarrow}(E) - \rho_{-}^{\leftarrow}(E) = -2m\nu \dot{X} \left(\frac{1 - g_0}{g_0 + g_1 - 2g_0 g_1} \right) \frac{\partial f(E)}{\partial E}$$
 (22)

and for the current we get

$$I = \int_0^\infty \frac{dp}{2\pi} (\rho_{\pm}^{\rightarrow} - \rho_{\pm}^{\leftarrow}) ev = \int_0^\infty \frac{dp}{2\pi} g_1(\rho_{+}^{\rightarrow} - \rho_{-}^{\leftarrow}) ev$$
 (23)

$$= -\dot{X} \int_0^\infty \left[\frac{e}{\pi} \left(\frac{(1 - g_0)g_1}{g_0 + g_1 - 2g_0 g_1} \right) \mathsf{m} v \right] \frac{\partial f(E)}{\partial E} dE \tag{24}$$

With the assumption of zero temperature Fermi occupation this gives the cited result for G^1 .

5. Classical derivation using the Kubo formula

The generalized fluctuation-dissipation version of the Kubo formula (see Ref.[4] and further references therein) relates the generalized conductance to the the cross correlation function of the current I and the generalized force $\mathcal{F} = -\partial \mathcal{H}/\partial X$. If X is the displacement X_1 of the scatterer then

$$\mathcal{F} = -\frac{\partial \mathcal{H}}{\partial X_1} = X_2 \delta'(x - X_1) \tag{25}$$

For the sake of comparison with previous results we assume zero temperature Fermi occupation. Then the Kubo formula takes the form

$$G = g(E_F) \int_0^\infty \langle I(\tau)\mathcal{F}(0)\rangle d\tau = \frac{L}{\pi\hbar v_F} \langle Q\mathcal{F}\rangle$$
 (26)

where $g(E) = L/(\pi\hbar v_F)$ is the density of states. This density of states is proportional to the total "volume" of the network which is L. In the second expression we got rid of the time by introducing the notation

$$Q = \int_0^\infty I(\tau)d\tau \tag{27}$$

It should be clear that both the generalized force \mathcal{F} and the transported charge Q are functions in phase space, and that $\langle ... \rangle$ stands for phase space average over position and velocity. For \mathcal{F} we already have an explicit expression Eq.(25). Now we have to figure out what is Q.

On the ring there are two scatterers, and one point $x = x_0$ where the current is measured. Hence the ring is divided into 3 segments. In addition, there are two possible directions of motion (clockwise, anticlockwise). Hence the phase space is divided into 6 regions. It is obvious that the outcome from Eq.(27) depends merely on which region the classical trajectory had started its journey in. In fact we need to consider only the 4 regions where

the particle starts in the vicinity of the moving scatterer, else \mathcal{F} vanishes. So we have the "+" region between the moving scatterer and x_0 , and the "-" region on the other side between the two scatterers. Accordingly the four possible outcomes from Eq.(27) are:

$$Q_{+}^{\rightarrow} = e \left[\frac{1}{2(1 - g_T)} \right] \tag{28}$$

$$Q_{+}^{\leftarrow} = -e \left[\frac{1}{2(1 - g_T)} - 1 \right] \tag{29}$$

$$Q_{-}^{\rightarrow} = \left[\frac{g_0}{1 - (1 - g_1)(1 - g_0)} - \frac{g_1(1 - g_0)}{1 - (1 - g_1)(1 - g_0)} \right] Q_{+}^{\rightarrow} = \frac{g_0 - g_1 + g_0 g_1}{g_0 + g_1 - g_0 g_1} Q_{+}^{\rightarrow}$$
(30)

$$Q_{-}^{\leftarrow} = -\frac{g_{1} - g_{0} + g_{0}g_{1}}{g_{0} + g_{1} - g_{0}g_{1}}Q_{+}^{\rightarrow}$$

$$(31)$$

The derivation of the above expressions is as follows. It is simplest if the particle starts in the "+" region, because then we can regard the two scatterers as one effective scatterer g_T . Assume that at time t=0 the particle approach $x=x_0$ from the left. The charge that goes through the section after a round trip is suppressed by a factor $(2g_T-1)$ due to the scattering (we sum the clockwise and the anticlockwise contributions). Thus we find that the total charge that goes through the section due to multiple reflections is a geometric sum that leads to Eq.(28). If we start in the "+" region in the opposite direction, then we have the same sequence but with the opposite sign and without the first term. Hence we get Eq.(29). Next assume that at t=0 the particle starts in the "-" region, and approaches g_0 from the left. Then we can have at a later time a positive pulse of current. The probability for that is the geometric summation over $g_0((1-g_0)(1-g_1))^{\text{integer}}$. Otherwise, we get a negative pulse of current, with a complementary probability that can be regarded as a geometric summation over $g_1((1-g_0)(1-g_1))^{\text{integer}}(1-g_0)$. Thus the total current through the section, taking into account all subsequent multiple reflections (rounds) is given by Eq.(30). A similar calculation leads to Eq.(31).

Since there are only four possible values for Q the calculation of the phase space average becomes trivial:

$$\langle Q\mathcal{F}\rangle = \frac{1}{2L} \left[\int_{+} \mathcal{F} dr \right] Q_{+}^{\rightarrow} + \frac{1}{2L} \left[\int_{+} \mathcal{F} dr \right] Q_{+}^{\leftarrow} + \frac{1}{2L} \left[\int_{-} \mathcal{F} dr \right] Q_{-}^{\rightarrow} + \frac{1}{2L} \left[\int_{-} \mathcal{F} dr \right] Q_{-}^{\leftarrow}$$

The integral over \mathcal{F} is taken either within the "+" or within the "-" region. It is trivially related to the momentum impact and yields the result

$$\int_{\pm} \mathcal{F} dr = \mp \mathsf{m} v_{\scriptscriptstyle F}^2 \tag{32}$$

Putting everything together we get the desired result for G^1 . With some minor modifications we can calculate G^2 using the same procedure.

6. The quantum mechanical picture

The Kubo formula holds also in the quantum mechanical case. But now I and \mathcal{F} are operators, so it is more convenient to express the Kubo formula using their matrix elements. After some algebra one obtains the result:

$$G = \sum_{m(\neq n)} \frac{2\hbar \text{Im}[I_{nm}] \mathcal{F}_{mn}}{(E_m - E_n)^2 + (\Gamma/2)^2}$$
(33)

For more details see Ref.[4] and further references therein. In the above formula it is assumed that only one energy level (n) is occupied. If we have zero temperature Fermi occupation, then

we have to sum over all the occupied levels. The Kubo formula incorporates a parameter Γ that reflects either the non-adiabaticity of the driving, or environmentally induced "memory loss" due to decoherence. For a strictly isolated system in the strict adiabatic limit we have $\Gamma = 0$. Then we identify G as an element of Berry's field B, as explained in the introduction. The effect of Γ on B will be discussed below.

We would like to see how the classical result can emerge in some limit from the above quantum expression. It turns out that this does not require a detailed calculation. We can use some topological properties of \boldsymbol{B} in order to figure out the answer! The main observations that we further explain below are:

- (1) The B is divergence-less with the exception of Dirac monopoles
- (2) The monopoles are arranged in \vec{X} space as vertical chains
- (3) The far field of B is like a two-dimensional electrostatic problem
- (4) Only non-compensated chains give net contribution

As long as the occupied level n does not have a degeneracy with a nearby level, B is finite and divergence-less. Only at degeneracies can it become singular. It can be argued that these singularities must have their charge quantized in units of $\hbar/2$ else the Berry phase would be ill defined. We have defined $X_3 = \Phi$ as the Aharonov-Bohm flux through the ring. This means that if we change X_3 by $2\pi\hbar/e$ then by gauge invariance we have another degeneracy. This means that the Dirac monopoles are arranged as vertical chains, and that the average charge per unit length is $e/(4\pi)$. Thus the far field of a Dirac chain is as in a two dimensional electrostatic problem. If we calculate the line integral of Eq.(1) then we get, within the framework of the far field approximation, Q = 1. Thus we conclude that if we have several Dirac chains of the same "sign", then Q simply counts how many are encircled.

We have to notice that if we have Fermi occupation, then the *net* contribution comes only from degeneracies of the last occupied level with the first unoccupied level. This is what we meant above (item 4) by "non-compensated". In order to avoid misunderstanding of the "compensation" issue let us discuss with some more details what happens if two neighboring levels n and m are occupied. With the level n we associate a field $\mathbf{B}^{(n)}$, while with m we associate a field $\mathbf{B}^{(m)}$. In general $\mathbf{B}^{(m)} \neq -\mathbf{B}^{(n)}$. If we are near a degeneracy than we may say that $\mathbf{B}^{(n)}$ emerges from a Dirac chain which is associated with level n, while $\mathbf{B}^{(m)}$ emerges from a Dirac chain which is associated with level n. By inspection of Eq.(33), taking into account that $\text{Im}[I_{nm}] = -\text{Im}[I_{mm}]$, we realize that the two Dirac chains have opposite charge. Their corresponding fields do not cancel each other, but the total field is no longer singular, implying that the *net* charge is zero.

In the quantum stirring problem we shall see that the X_1 distance between non-compensated chains is simply half the De-Broglie wavelength $\lambda_E = 2\pi/k_E$. From this it follows that the amount of charge which is pushed by a very "large" scatterer is

$$Q \approx e \frac{\Delta X_1}{\lambda_E/2} = e \frac{k_E}{\pi} \times \Delta X_1 \tag{34}$$

What happens if the cycle is not in the "far field" but rather passes through the distribution of the monopoles? To be more specific let us consider what happens to Q if we displace the scatterer a distance ΔX_1 . What is the dependence on X_2 ? Do we get the classical result as in Fig.5? Obviously, in order to get the classical result the distribution $\sigma(X_1, X_2)$ should be in accordance with Eq.(15). Strictly speaking this is *not* the case because we have a discrete set of monopoles rather than a smooth distribution of "magnetic charge". Still we can hope that $\sigma(X_1, X_2)$ would be classical-like upon course graining. We discuss further this issue in the next paragraphs.

If we make a pumping cycle in the vicinity of a monopole then it is obvious that the result would be very different from the classical prediction. What we expect to get in the quantum mechanical case is illustrated in the upper panel of Fig.7. For a cycle that goes very close to a monopole the charge can be huge. In reality it is very difficult to satisfy the adiabatic condition near a degeneracy, or else there are always environmental effects. Either way, once we have a finite Γ , the result that we get for Q is smoothed.

If the pumping cycle passes through a distribution of many monopoles then what we expect to get (as we deform or shift the cycle) are huge fluctuations as illustrated in the lower panel of Fig.7. Again, the effect of either non-adiabaticity or environmental effects is to smooth away these fluctuations. The interested reader can find some further discussion of this point including a numerical example in [12].

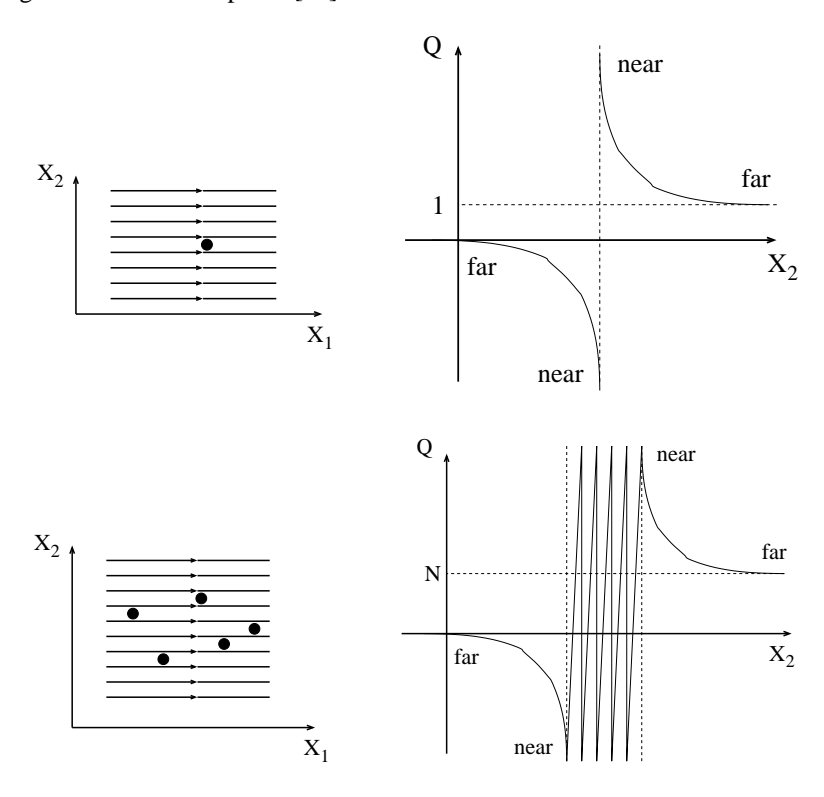


Fig.7. Several pumping cycles are indicated in the left panels: It is implicit that each segment is closed as in Fig.3. The black points represent degeneracies. For each pumping cycle one can calculated Q. The qualitative expectation for the outcome is illustrated in the right panels. In the upper illustration we assume that the pumping cycle encircles only one degeneracy, while in the lower illustration we assume that it encircles N degeneracies. In a later section we display numerical results that support the illustrated expectations.

Coming back to the quantum-classical correspondence (QCC) issue, we realize that at best QCC can be satisfied in a statistical sense. So we ask whether the coarse grained $\sigma(X_1, X_2)$ agrees with the classical expectation Eq.(15). The answer which we give in the following sections, is that QCC is not realized in the case of simple non-chaotic models. In the "simple" cases we get a non-classical $\sigma(X_1, X_2)$ and hence a different dependence of Q on X_2 .

7. The degeneracies in X space

We can use the scattering approach in order to find the energy levels of a ring. In this approach the ring is opened at some arbitrary point and the *S* matrix of the open segment is specified. It is more convenient to use the row-swapped matrix, such that the transmission amplitudes are along the diagonal:

$$\tilde{\mathbf{S}}(E; X_1, X_2) = e^{i\gamma} \begin{pmatrix} \sqrt{g} e^{i\phi} & i\sqrt{1 - g} e^{-i\alpha} \\ i\sqrt{1 - g} e^{i\alpha} & \sqrt{g} e^{-i\phi} \end{pmatrix}$$
(35)

The periodic boundary conditions imply the following secular equation

$$\det(\tilde{\mathbf{S}}(E; X_1, X_2) - \mathbf{1}) = 0 \tag{36}$$

Using

$$\det(\tilde{\mathbf{S}} - I) = \det(\tilde{\mathbf{S}}) - \operatorname{trace}(\tilde{\mathbf{S}}) + 1 \tag{37}$$

$$\det(\tilde{\mathbf{S}}) = (e^{i\gamma})^2 \tag{38}$$

$$\operatorname{trace}(\tilde{\mathbf{S}}) = 2\sqrt{g}e^{i\gamma}\cos\phi \tag{39}$$

we get

$$\cos(\gamma(E)) = \sqrt{g(E)}\cos(\phi) \tag{40}$$

In order to find the eigen-energies we plot both sides as a function of E. The left hand side oscillates between -1 and +1, while the right hand side may have a smaller amplitude. It is not difficult to realize that the only way to have two eigen-energies coincide is to get

$$\left\{ \begin{array}{lll}
\phi & = & 0 \mod(2\pi) \\
g & = & 1 \\
\gamma & = & n_{\text{even}}\pi
\end{array} \right\} \qquad \text{or} \qquad \left\{ \begin{array}{lll}
\phi & = & \pi \mod(2\pi) \\
g & = & 1 \\
\gamma & = & n_{\text{odd}}\pi
\end{array} \right\} \tag{41}$$

where n is either even or odd integer that can be exploited (if we keep track over γ) as a level counter.

Both g and γ depend on $(E; X_1, X_2)$. Since we want g to be maximal the condition for having a degeneracy involves 4 rather than 3 equations as we are going to see below. An immediate conclusion is that we have two types of Dirac chains: those that have monopoles in the plane of the pumping cycle $(X_3 = \Phi = 0)$, and the others that have monopoles off the plane of the pumping cycle.

In our model system we have two scatterers. One is the moving scatterer and the other is the rest of the network. The two are connected by arms of length $L_A - X_1$ and $L_B + X_1$. The constants L_A and L_B can be absorbed into the definition of the surrounding network. Each scatterer is fully characterized by the set of parameters $\{g_i, \gamma_i, \alpha_i, \phi_i\}$. Note that we do not absorb X_1 into the definition of α_0 . After some algebra we find the following expressions for the transmission coefficient and for the total phase shift:

$$g = \frac{g_0 g_1}{2 - g_0 - g_1 + g_0 g_1 + 2\sqrt{(1 - g_0)(1 - g_1)}\cos(\gamma_0 + \gamma_1 + \alpha_0 + \alpha_1 - 2k_E X_1)}$$
(42)

$$\gamma = \gamma_0 + \gamma_1 \tag{43}$$

where k_E is the wavenumber that corresponds to the energy E. Thus the conditions for having a degeneracy take the form

$$\begin{cases} X_3 = \text{integer flux} \\ g_0(X_2) = g_1 \\ \alpha_0 + \alpha_1 - 2k_E X_1 = \pi \mod(2\pi) \\ \gamma_0 + \gamma_1 = n_{\text{even}} \pi \end{cases} \begin{cases} X_3 = \text{half integer flux} \\ g_0(X_2) = g_1 \\ \alpha_0 + \alpha_1 - 2k_E X_1 = 0 \mod(2\pi) \\ \gamma_0 + \gamma_1 = n_{\text{odd}} \pi \end{cases}$$
(44)

We have highlighted the dependence on the parameters (X_1, X_2, X_3) . There is of course also an implicit dependence of $\{g_i, \gamma_i, \alpha_i\}$ on the energy E. The conditions that are listed above are very intuitive: The system should have time reversal symmetry; The barriers should "balance" each other; The phases which are associated with the reflections should lead to destructive interference; And the total phase shift should respect the periodic boundary conditions.

From Eq.(44c) we see that in general the X_1 distance between degeneracies that belong to the same level is roughly half the De-Broglie wavelength as stated previously. The question that we would like to address is how these degeneracies are distributed with respect to X_2 .

8. Quantum stirring in simple rings

We would like to find the distribution of degeneracies with respect to X_2 in the simplest model: a ring with two delta scatterers (see Fig.1). The arms that connect the two scatterers are of length $L_A + X_1$ and $L_B - X_1$. For the S matrix that represents the fixed scatterer (including the arms) we have

$$g_1(E) = \left[1 + \left(\frac{\mathsf{m}}{\hbar^2 k_{\rm F}}V\right)^2\right]^{-1}$$
 (45)

$$\gamma_1(E) = k_E(L_A + L_B) - \arctan\left(\frac{\mathsf{m}}{\hbar^2 k_{\scriptscriptstyle F}} X_2\right) \tag{46}$$

$$\alpha_1(E) = k_E(L_A - L_B) \tag{47}$$

Since the dependence of g_0 and g_1 on the barrier "size" has the same functional form, the condition Eq.(44c) implies $X_2 = V$ irrespective of E. Thus we get that all the degeneracies are concentrated at the same X_2 . This is clearly very different from the classically expected distribution.

In Fig.8 we display an example. The degeneracies that are associated with the first 7 levels are indicated. Filled circles stand for $\phi = 0$ degeneracies, while hollow circles stand for $\phi = \pi$ degeneracies. Only the last (7th) level contributes non-compensated monopoles. The X_1 distance between the non-compensated monopoles is roughly half De-Broglie wavelength.

In Fig.9 we show what happens to the degeneracies if we add a second fixed scatterer. We have chosen an additional scatterer that can be treated as a perturbation. The calculation was done using perturbation theory. We shall not present the details of this lengthy calculation here. For larger perturbations (not presented) we had to solve the secular equation numerically. This was done using an efficient algorithm [19]. In any case, the purpose of Fig.9 is merely to demonstrate that once the symmetry of the system is broken the degeneracies spread out in the X_2 direction.

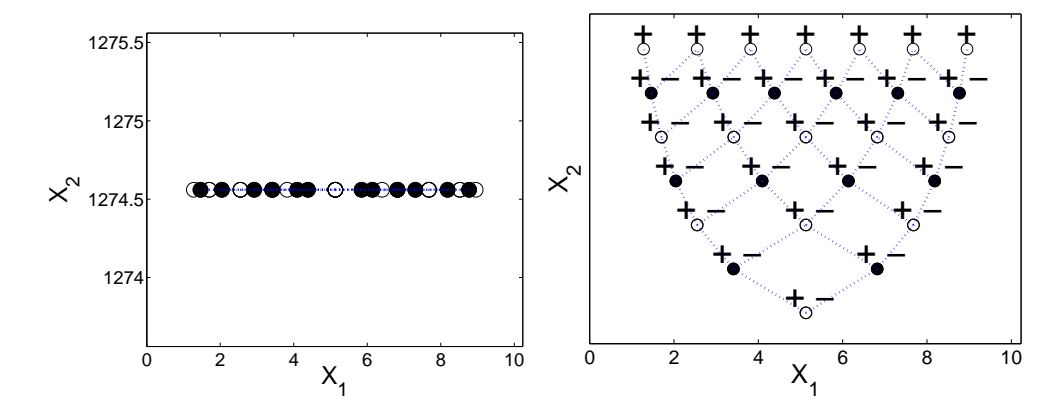


Fig.8. The degeneracies in the double delta model of Fig.1. We set $L_A=10.23$ and $L_B=0$, so that X_1 measures the distance from the fixed scatterer. The "size" of the fixed delta scatterer is V=1274.56. We use units such that $m=\hbar=1$. We assume that only the lower 7 levels are occupied. The filled circles are degeneracies on the flux zero plane and the empty circles are degeneracies on the flux π plane. The left graph shows the actual arrangement in the (X_1, X_2) plane. Namely, all the degeneracies are on the line $X_2=V$. In the right graph the degeneracies were displaced for the sake of clarity. Only the 7th occupied level contributes non-compensated monopoles.

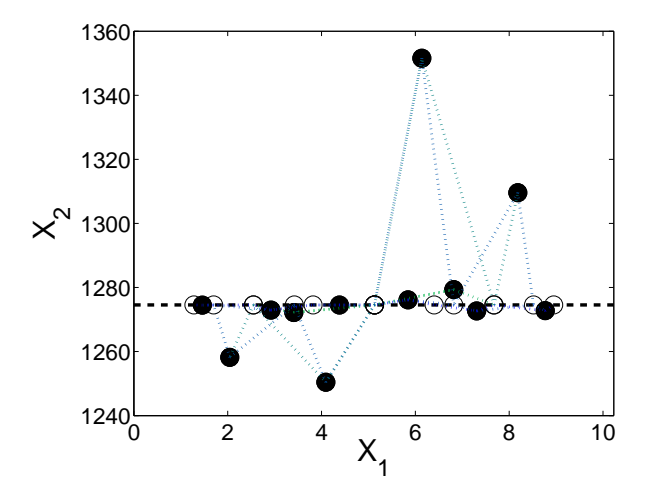


Fig.9. The degeneracies in the triple delta model of Fig.1. Namely, to the model of Fig.8 we have added a delta barrier of "size" $V_P = 10^{-5}$, located at x = 7.61. This additional delta barrier can be treated as a small perturbation. As a result of this perturbation the degeneracies shift and spread out in the X_2 direction. Degeneracies that belong to the same level are connected by a line. As in the previous figure only the 7th occupied level contributes non-compensated monopoles.

The distribution $\sigma(X_1, X_2)$ in the case of a ring with a single fixed scatterer is very different from the classical prediction. Consequently also Q comes out very different from Eq.(15) [and see also Fig.6]. The reader might be curious to know how Q depends on the "size" (X_2) of the scatterer in the case of Fermi occupation. So we have calculated G numerically using Eq.(33), and integrated over it to get Q. The numerical results are displayed in Fig.10. Further analysis of the crossover from "near field" to "far field" cycles will be published in a separate work [17].

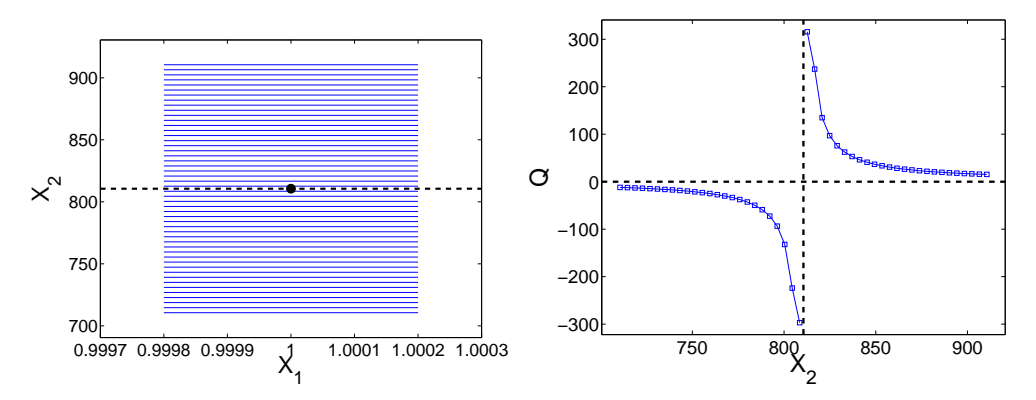


Fig.10. Several pumping routes are displayed in the left panel. For each of them Q has been calculated numerically. The results are displayed in the right panel. Note the agreement with the qualitative expectation that has been expressed in Fig.7. The calculation is done for the double delta model of Fig.1 with $L_A = 1000.23$ and $L_B = 0$. The "size" of the fixed barrier is V = 810.56. The energy level involved are n = 998 and m = 999. We use units such that $m = \hbar = 1$.

9. Quantum stirring in chaotic rings

We would like to find the distribution of degeneracies with respect to X_2 in case of a chaotic network (see an example in Fig.1). Let us try to extend the approach that has been used in the previous section. A hypothetical illustration of $g_1(E)$ in the chaotic case is displayed in Fig.11. The universal conductance fluctuations of g_1 are characterized by a one parameter probability distribution $P(g_1; \bar{g}_1)$ which we discuss below. This probability distribution depends on one parameter, which we choose to be the average transmission \bar{g}_1 .

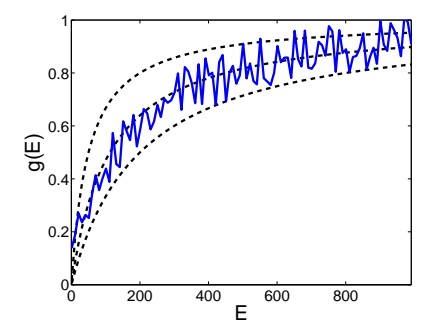


Fig.11. A hypothetical illustration of $g_1(E)$ in the case of a complex "chaotic" barrier. Such a barrier can be modeled as a network (Fig.1a), or it can be characterized using random matrix theory. The smooth curves are the transmission $g_0(E; X_2)$ of the delta scatterer for 3 different values of X_2 .

In order to get a degeneracy, a necessary but insufficient condition is that the transmission of the two barriers is equal $(g_0(E; X_2) = g_1(E))$. The solution of this equation can be determined graphically via Fig.11. In fact in most practical applications we can assume that our interest is restricted to some small energy window such that the smooth E dependence of g_0 can be neglected. So the equation is in fact $g_0(X_2) = g_1(E)$. For a given E we can find an $X_2^{(E)}$ such that this equation is satisfied. By playing with X_1 we can satisfy the α related phase condition for having a degeneracy. But we still have to satisfy also the γ related phase

condition, which leads to the quantization of the energy E. Hence the erratic $X_2^{(E)}$ is sampled. Still it is reasonable to assume that the distribution of the so-obtained X_2 values is not affected by this random-like sampling. We therefore conclude the following relation:

$$Prob\left[X_{2} < X_{2}^{(E)} < X_{2} + dX_{2}\right] = Prob\left[g_{0}(X_{2}) < g_{1} < g_{0}(X_{2} + dX_{2})\right]$$
(48)

This implies a simple relation between $\sigma(X_1, X_2)$ and the probability function $P(g_1; \bar{g}_1)$

$$\sigma(X_1, X_2) = \text{const} \times \frac{dg_0(X_2)}{dX_2} P(g_0(X_2))$$
(49)

Thus the problem of finding $\sigma(X_1, X_2)$ has reduced to the problem of finding $P(g_1; \bar{g}_1)$.

We can now proceed in three directions: (A) To determine P() from simple heuristic quantum chaos considerations; (B) To determine P() from formal random matrix theory considerations; (C) To use reverse engineering in order to determine what is P() that would give the classical result. It should be clear that universality can be expected only if $\bar{g}_1 \ll 1$. In Fig.12 we make a comparison between the outcomes of these three procedures for $\bar{g}_1 = 0.001$. In the following paragraph we give the details of the calculation.

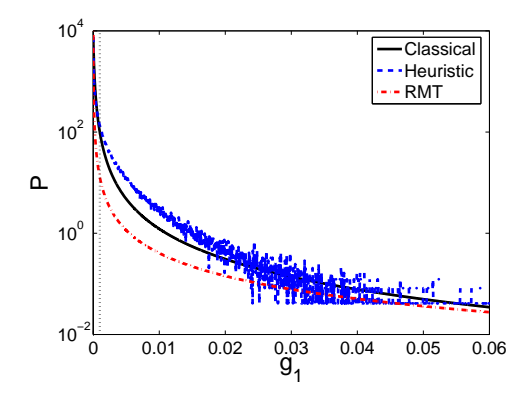


Fig.12. A plot of the distribution $P(g_1; \bar{g}_1)$ according to several different expressions. In this calculation we assume that the average transmission is $\bar{g}_1 = 0.001$, which is represented in the figure by a vertical dashed line. The "heuristic" result is based on sampling of the random variable $g_1 = \bar{g}_1 \eta_1 \eta_2$ where η is Porter-Thomas distributed. The "RMT" result is based on Eq.(50). The "classical" result is based on Eq.(51).

The heuristic approach is based on the idea that the transmission via a chaotic network depends on the amplitudes of the wavefunctions at the entrance and exit points. One might expect $g_1 = \bar{g}_1 \eta_1 \eta_2$, where η has the Porter-Thomas distribution [20] $P_{\text{GOE}}(\eta) = (1/\sqrt{2\pi\eta}) \mathrm{e}^{-\eta/2}$. This leads to the "heuristic" result in Fig.12. In fact this result should not be taken too seriously. The formal RMT calculation [21] of the probability distribution $P(g_1; \bar{g}_1)$ leads to the following expressions:

$$P_{\text{RMT}}(g_1; \bar{g}_1) = \begin{cases} (2/\pi^2 \bar{g}_1) g_1^{-1/2} & \text{for } g_1 \ll (\bar{g}_1)^2 \ll 1\\ (4\bar{g}_1/\pi^2) g_1^{-3/2} & \text{for } (\bar{g}_1)^2 \ll g_1 \ll 1 \end{cases}$$
(50)

The small g_1 approximation is universal: it merely assumes that the system has time reversal symmetry. It has been confirmed [22] that this universal behavior holds also for network systems. But for larger values of g_1 there are deviations that has to do with semiclassical considerations. It is therefore in the latter region where one might expect quantum-classical correspondence.

The probability distribution $P(g_1; \bar{g}_1)$ that would reproduce the classical result Eq.(15) via Eq.(49) is:

$$P_{\rm CL}(g_1; \bar{g}_1) = \frac{(1 - g_1^{cl})g_1^{cl}}{(g_1 + g_1^{cl} - 2g_1g_1^{cl})^2}$$
(51)

with $g_1^{cl} \approx 0.12 \bar{g_1}$. In order to compare with the RMT result we note that

$$P_{\text{CL}}(g_1; \bar{g}_1) \approx \begin{cases} (1/g_1^{cl}) (1 - 2g_1/g_1^{cl}) & \text{for } g_1 \ll g_1^{cl} \ll 1\\ g_1^{cl} g_1^{-2} & \text{for } g_1^{cl} \ll g_1 \ll 1 \end{cases}$$
(52)

We see that in the large g_1 region, where one might expect quantum-classical correspondence, there is no agreement between $P_{\text{CL}}()$ and $P_{\text{RMT}}()$. We suspect that $P_{\text{RMT}}()$ cannot be trusted there. Otherwise we have to conclude that Eq.(49) fails to take into account strong correlations in the arrangement of Dirac monopoles. Either way it seems that RMT alone is not enough in order to reproduce the classical result.

10. The emergence of the classical limit

With simple minded RMT reasoning we have failed to get a quantitative correspondence with the classical result. We therefore look for a different way to get an estimate for either B_2 or $\sigma(X_1, X_2)$ in the case of a chaotic network. One obvious way is to use the result of Ref.[23] regarding the distribution of degeneracies (diabolic points). The perturbation term which is associated with X_2 is

$$W = \frac{\partial \mathcal{H}}{\partial X_2} = \delta(x - X_1) \tag{53}$$

and the density of the degeneracies should be [23]

$$\sigma(X_1, X_2) = \frac{\pi}{3} g(E)^2 RMS[\mathcal{F}_{nm}] RMS[\mathcal{W}_{nm}] \propto RMS[\mathcal{W}_{nn}]$$
 (54)

where g(E) is the density of states. In the first equality it is implicit that the root mean square (RMS) of *near diagonal* matrix elements should be estimated. In fact only RMS[W_{nm}] is required in order to find the X_2 dependence. For a quantum chaos system with time reversal symmetry the variance of the near diagonal elements equals half the variance of the diagonal elements [24], leading to the second expression.

There is a well known semiclassical recipe [25, 26] for calculating the variance of the near diagonal matrix elements W_{nm} . One should find the classical correlation function $C(\tau) = \langle W(t)W(0) \rangle - \langle W \rangle^2$, and then integrate over τ . If W were the current operator then $\langle W \rangle$ would be equal to zero, and we could proceed as in section 5. But in case of Eq.(53) there is a problem: The sign of W(t) does not fluctuate, and it is essential to take into account the distribution of the delay times inside the network. Therefore there is no obvious relation to the transmissions g_0 and g_1 .

An optional possibility is to try to evaluate RMS[W_{nn}], where $W_{nn} = |\psi_{\text{barrier}}|^2$ is the "intensity" of the wavefunction at the location of the scatterer. Obviously the result depends on both g_0 and g_1 , and requires considerations which are at least as difficult as estimating universal conductance fluctuations. So it seems that we would run into the same problems as in the previous section.

Still there is the option to calculate $G^1 = \mathbf{B}_2$ from the Green function of the system. This has been done in [12]: Writing the Green function as a sum over trajectories, we have expressed G^1 as a double sum over paths. If this double sum is averaged over the energy one obtains the diagonal approximation, leading to the classical result. At first glance the energy

averaging is not quite legitimate, because the energy is quantized. But one can justify this procedure in the case of a "quantum chaos system". We have further supported this claim by the numerical analysis of the chaotic network of Fig.1 [12]. We therefore conclude that for a chaotic network the distribution of degeneracies should be in accordance with Eq.(15).

11. Conclusions

As we translate a scatterer of "size" X_2 a distance ΔX_1 along a single mode wire, the amount of charge which is pushed is

$$Q = r(X_2) \times \frac{e}{\pi} k_{\scriptscriptstyle F} \times \Delta X_1 \tag{55}$$

where k_F is the Fermi momentum. If the scatterer is very "large" $(X_2 \to \infty)$ then we expect to have $r(X_2) = 1$. This expectation is based on the "snow plow" picture that has been explained in the conclusion of section 2. This result is also confirmed by the formal BPT based calculation in the case of an *open* geometry. It also can be formally derived for a *closed* geometry using the "Dirac chains picture". In the latter case the key observation is that the X_1 distance between contributing degeneracies is roughly half the De-Broglie wavelength. See Eq.(34).

Next we ask what happens to $r(X_2)$ as X_2 becomes smaller. In the case of an *open* geometry the intuitive naive guess, which is based on the "snow plow" picture, turns out to be correct. Namely, $r(X_2) = 1 - g_0$ is simply the reflection coefficient: Some of particles are not "pushed" by the scatterer because of its partial transparency. In the case of a *closed* geometry we have shown that the *classical* result for $r(X_2)$ is modified: now it depends also on the overall transmission of the device. See Eq.(13).

It is important to realize that the *classical* result for $r(X_2)$ is in complete agreement with the common sense expectation. Namely, we have $0 < r(X_2) < 1$, and the dependence on the "size" of the scatterer is monotonic. But once we go to the quantum mechanical analysis we have a surprise. The results that we get are counter-intuitive. They are most puzzling (Fig.10) in the case of the simplest model, in which the ring contains only one fixed delta barrier (V). As we decrease X_2 the transported charge Q becomes larger(!). Moreover, once X_2 becomes smaller than V, the coefficient $r(X_2)$ changes sign. This means that as we push the particles "forward" the current is induced "backwards".

The reason for the failure of our intuition is our tendency to regard "adiabatic transport" as a zero order adiabatic approximation, while in fact it is based on a first order analysis (for a detailed discussion see section 4 of [17]). As a parameter in the system is changed, the induced current can be in either direction.

In order to understand the route towards quantum-classical correspondence it is essential to figure out how the degeneracies spread out in \vec{X} space. As the system becomes more complex, we get for $r(X_2)$ a result that resembles the classically implied one. The resemblance is at best only on a coarse grained scale: the quantum result has strong fluctuations. These are related to universal conductance fluctuations.

We have made an attempt to deduce from RMT considerations the "chaotic" distribution of the degeneracies, and hence the dependence of $r(X_2)$ on X_2 . The quantitative results do not agree. We therefore suspect that RMT considerations alone are not enough in order to establish quantum-classical correspondence. Rather we had used [12] semiclassical tools in order to establish this correspondence.

Acknowledgments

We thank Nir Davidson for illuminating us regarding the feasibility of measuring neutral currents in cold atom systems. We also had the pleasure to have very helpful discussions with Itamar Sela, Tsampikos Kottos, Holger Schanz and Michael Wilkinson. This research was supported by the Israel Science Foundation (grant No.11/02), and by a grant from the GIF, the German-Israeli Foundation for Scientific Research and Development.

References

- [1] M.V. Berry, Proc. R. Soc. Lond. A 392 (1984) 45.
- [2] M.V. Berry and J.M. Robbins, Proc. R. Soc. Lond. A 442 (1993) 659.
- [3] D. Cohen, Phys. Rev. B 68 (2003) 155303.
- [4] For a mini-review and further references see: D. Cohen, Physica E 29, 308 (2005).
- [5] M. Büttiker et al, Z. Phys. B-Condens. Mat., 94 (1994) 133.
- [6] P. W. Brouwer, Phys. Rev. B 58 (1998) R10135.
- [7] D. Cohen, Phys. Rev. B 68 (2003) 201303(R).
- [8] D. Cohen, Solid State Communications 133, 583 (2005).
- [9] D. J. Thouless, Phys. Rev. B27 (1983) 6083.
- [10] J.E. Avron et al, Rev. Mod. Phys. 60 (1988) 873.
- [11] J. E. Avron et al, Phys. Rev. B 62, R10 (2000) 618.
- [12] D. Cohen, T. Kottos and H. Schanz, Phys. Rev. E 71, 035202(R) (2005).
- [13] B. Reulet M. Ramin, H. Bouchiat and D. Mailly, Phys. Rev. Lett. 75, 124 (1995).
- [14] C.F. Bharucha, J.C. Robinson, F.L. Moore, K.W. Madison, S.R. Wilkinson, Bala Sundaram, and M.G. Raizen, Atomic Physics 15, 62 (World Scientific, Singapore, 1997). V. Milner, J.L. Hanssen, W.C. Campbell, and M.G. Raizen, Phys. Rev. Lett. 86, 1514 (2001).
- [15] N. Friedman, A. Kaplan, D. Carasso, and N. Davidson, Phys. Rev. Lett. 86, 1518 (2001). M. Andersen, and N. Davidson, Phys. Rev. Lett. 87, 274101 (2001).
- [16] I. Bialynicki-Birula and Z. Bialynicka-Birula, Phys. Rev. Lett. 78, 2539 (1997).
- [17] I. Sela and D. Cohen, cond-mat/0512500.
- [18] D. Cohen and Y. Etzioni, J. Phys. A 38, 9699 (2005).
- [19] We thank H. Schanz for suggesting the numerical algorithm.
- [20] F. Haake, Quantum Signatures of Chaos (Springer 2001).
- [21] P.W. Brouwer and C.W.J. Beenakker, Phys. Rev. B. 50, 11263 (1994).
- [22] T. Kottos and U. Smilansky, J. Phys. A 36, 3501-3524 (2003).
- [23] M. Wilkinson and E. J. Austin, Phs. Rev. A 47, 4 (1993).
- [24] B. Eckhardt, S. Fishman, J. Keating, O. Agam, J. Main and K. Muller, Phys. Rev. E 52, 5893 (1995); and further references therein.
- [25] M. Feingold and A. Peres, Phys. Rev. A 34 591, (1986).
- [26] M. Feingold, D. Leitner, M. Wilkinson, Phys. Rev. Lett. 66, 986 (1991).